Evidence for 2D Precursors and Interdiffusion in the Evolution of Self-Assembled CdSe Quantum Dots on ZnSe

C. S. Kim,[1] M. Kim,[1] J. K. Furdyna,[1] M. Dobrowolska,[1,*] S. Lee,[2] H. Rho,[3] L. M. Smith,[3] Howard E. Jackson,[3] E. M. James,[4] Y. Xin,[4] and N. D. Browning[4]

[1]*Department of Physics, University of Notre Dame, Notre Dame, Indiana 46556*
[2]*Department of Electronic Materials Engineering, Kwangwoon University, Seoul, 139-701 Korea*
[3]*Department of Physics, University of Cincinnati, Cincinnati, Ohio 45221*
[4]*Department of Physics, University of Illinois at Chicago, Chicago, Illinois 60607*

(Received 22 December 1999)

The evolution of self-assembled CdSe quantum dots deposited on (and subsequently capped by) ZnSe was investigated on a series of samples grown by molecular beam epitaxy, with CdSe coverages from 0.5 to 2.6 monolayers. The samples were investigated by cross-sectional scanning transmission electron microscopy, as well as macro- and microphotoluminescence. The results clearly indicated a coexistence of 2D ZnCdSe platelets and 3D islands, showing clearly that the platelets act as precursors for the formation of the 3D islands.

PACS numbers: 78.66.Hf, 68.65.+g, 73.61.Ga, 81.15.Aa

It is now well established that lattice mismatched heteroepitaxy can lead to the formation of self-assembled quantum dots (QDs) [1]. The most extensive studies in this context have been carried out on InAs overlayers deposited epitaxially on [001] GaAs, for which the lattice mismatch is 7.1%. In the case of InAs QDs on GaAs it is usually assumed that coherent islands form after deposition of a "wetting layer" corresponding to 1 to 2 monolayers of InAs. However, a number of recent studies have shown that the growth mode is more complex, and is very sensitive to deposition conditions [2–4]. These aspects of self-assembled QD formation have generated much interest in the theoretical community [5–8]. Here one of the central challenges is to identify the dynamics of how exactly the initial (essentially 2D) pseudomorphic growth transforms into the final 3D-island formation.

One of the mechanisms by which the self-assembled QDs can form was proposed by Priester and Lannoo [9] who showed that the existence of a narrow distribution of sizes and shapes in the dot population can be explained by the formation of stable 2D platelets that act as precursors for the formation of coherent 3D islands. These authors predict that such platelets grow with increasing coverage until they reach some limiting distribution, and at that point spontaneously transform into 3D islands with the same distribution.

In this Letter we describe the evolution of self-assembled CdSe QDs deposited on—and subsequently capped by—ZnSe for a series of CdSe coverages, from 0.5 to 2.6 monolayers. The CdSe/ZnSe materials combination [10–12] is interesting because the lattice mismatch of CdSe on [001] ZnSe (7%) is practically identical to that of the InAs/GaAs combination [1]. However, processes such as surface diffusion, bond ionicity, and bulk interdiffusion—all of which affect QD formation—are element specific, and are therefore expected to result in differences between the self-assembly of CdSe/ZnSe and InAs/GaAs, despite their identical strain configurations.

The samples which we investigated were grown by molecular beam epitaxy (MBE) in a Riber 32 R&D MBE machine equipped with elemental sources. A ZnSe buffer was first grown at 300 °C on (100) GaAs substrates to a thickness of approximately 2 μm. During the growth of ZnSe the reflection high-energy electron diffraction (RHEED) pattern showed a consistently streaky 2×1 reconstruction throughout ZnSe deposition, together with well resolved RHEED oscillations of the specular spot. We take this to be a strong indication of layer-by-layer growth, and thus of a smooth ZnSe surface, with little or no surface roughness when the ZnSe growth was interrupted for subsequent CdSe deposition. For depositing CdSe the substrate temperature was raised to 350 °C. For the present study we have grown nine specimens, with nominal thicknesses of CdSe ranging from 0.5 to 2.6 monolayers. CdSe was deposited at a very slow rate of 14 sec/ML. After deposition of the CdSe layers the growth was interrupted for 2 sec, and CdSe was then capped (at the same 350 °C) by 50 nm of ZnSe.

The samples with 1.5 and 2.6 monolayer coverages of CdSe were then investigated using the Z-contrast imaging technique [13] in a JEOL 2010F scanning transmission electron microscope (STEM) [14]. Samples for cross-sectional STEM measurements were thinned to below 50 nm. The advantage of using this technique over conventional TEM methods is that the generated image is largely incoherent in nature, with the contrast being primarily dependent on the atomic number Z of the atoms under the electron probe [15]. For crystalline materials in zone-axis orientations, where the probe size (0.13 nm) is smaller than the atomic spacing, an element-specific compositional map can thus be generated with atomic resolution. For the ZnSe/CdSe system studied here, the

 0031-9007/00/85(5)/1124(4)$15.00

0.13 nm size of the microprobe means that the 0.14 to 0.16 nm spacings along the [110] direction are readily resolved, and the spatial map of the Cd-containing layer can be directly imaged.

Figure 1(a) shows a high resolution cross-sectional Z-contrast image of the sample with 1.5 monolayer coverage of CdSe. As seen from the contrast (color) variations in the image, the CdSe-containing layer is not uniform even at this low coverage, areas with high Cd concentration (red/yellow spots) being separated by "flat" regions with lower Cd content. Note that there is very little distortion of the lattice fringes in the region of the CdSe layer. This suggests that even the areas of higher Cd concentration are composed of CdZnSe rather than pure CdSe (i.e., there is a reduction in the lattice mismatch between the islands and their environment). The islands themselves vary in size both laterally and in the growth (up) direction; and we can clearly see the coexistence of both 3D and 2D islands. In particular, there are Cd-rich regions with large width-to-height ratios, which can be regarded as 2D platelets. We also notice the existence of one 3D island [on the left in Fig. 1(a)] with a diameter of about 8 nm and height of about 5 nm, which can be identified as a quantum dot. One can also notice another dot (second from the right) which is just in the process of expanding from a 2D platelet along the vertical direction. To our knowledge this is the first image which captures the onset of QD formation in the case of CdSe/ZnSe, clearly showing that the 2D island acts as a precursor to the formation of a 3D island.

Another important feature revealed by Fig. 1(a) is that the dots extend to the same degree above *and below* the interface. This is seen both for the fully developed dot (first on the left), and for the one in the process of forming, where it clearly starts to expand in both "up" and "down" directions. This is direct graphic evidence that interdiffusion plays an important role in the dynamics of quantum dot formation. Here it is important to remember that, for the experimental conditions used in the STEM measurement [14], the contrast in the image is dominated by *chemical* composition (i.e., by the atomic number, Z); thus, although the detector geometry cannot totally remove the residual coherent effects caused by strain at the interface [16], the images are primarily a map of the Cd distribution.

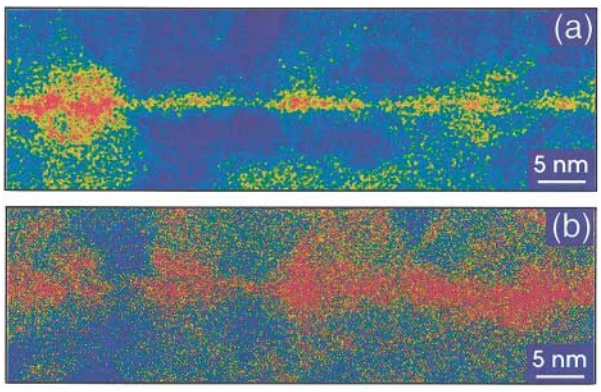

FIG. 1 (color). Cross-sectional high resolution Z-contrast images of samples with (a) 1.5 and (b) 2.6 monolayers of CdSe deposited on ZnSe, and capped. The pictures were digitally color-coded based on the contrast information in the STEM images: red corresponds to regions richest in Cd, blue to those richest in Zn. The growth direction is vertically "up."

Figure 1(b) shows a high resolution cross-sectional Z-contrast image for CdSe coverage of 2.6 monolayers. Here the image shows well formed 3D islands approximately 6 to 8 nm in diameter, extending up and down in the vertical (growth) direction. The fact that the STEM distortion of the lattice fringes in the region of the dots is now more pronounced suggests that the lattice mismatch is greater, and that at this coverage the dots (although still composed of CdZnSe) are now richer in Cd than in the case of 1.5 monolayer CdSe coverage.

Our STEM data are consistent with cross-sectional transmission electron microscopy (TEM) measurements performed on samples with 1.0 and 0.7 monolayer coverage of CdSe by other groups [11,17,18]. In those studies, as in ours, the pictures do not show a uniform wetting layer, but also reveal fluctuations of composition in the form of 2D islands with large width-to-height ratios. These results show that 2D ZnCdSe platelets form as soon as CdSe deposition begins (i.e., without forming a "true" wetting layer), and, as the deposition of Cd continues, the platelets grow at first laterally, and eventually (at the coverage of ca. 1.5 ML) vertically.

Macro- and microphotoluminescence measurements on these samples also corroborate the intriguing transition from 2D to 3D growth regimes seen in the STEM studies described above. Figure 2 shows microphotoluminescence spectra observed on five samples with different CdSe coverages, as indicated. One can see a clear progression of the spectrum toward lower energy as the CdSe coverage increases from 0.5 to 2.6 monolayers. Superimposed on the broad luminescence we observe sharp lines with typical widths of 200 μeV. Although the number of these sharp spikes decreases with decreasing CdSe coverage, it is important to note that the sharp lines are seen on *all* samples, including the one with CdSe coverage of only 0.5 monolayers.

In Fig. 2(b) we examine more closely the photoluminescence spectrum from the sample with 0.5 monolayers coverage (note the expanded scale). The emission as a whole exhibits a narrow 5 meV wide line shape having a weak low-energy tail, with a small number of narrow spikes superimposed on the tail. The tail itself arises from potential variations resulting from the fluctuation of CdSe concentration in the layer plane [19–21]. The spikes seen on the tail in the microphotoluminescence data for the sample with CdSe coverage of 0.5 monolayers thus correspond to individual potential fluctuations. When we proceed to the

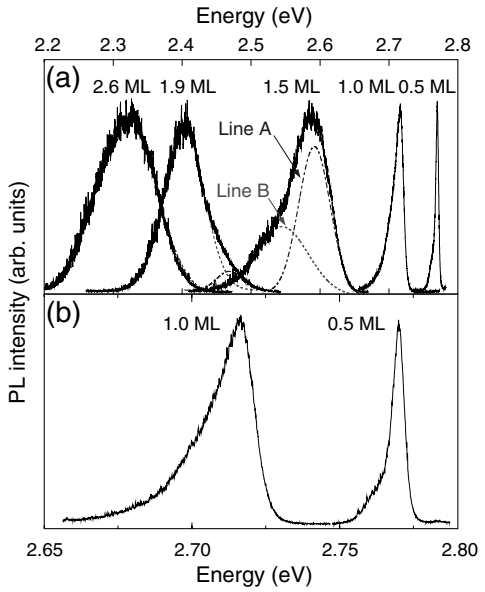

FIG. 2. (a) Microphotoluminescence spectra taken at 6 K on capped CdSe/ZnSe QD samples with different CdSe coverages (solid curves), together with best-fit simulations (dotted curves). (b) Microphotoluminescence spectra for samples with 0.5 and 1.0 monolayer coverage, plotted on an expanded energy scale.

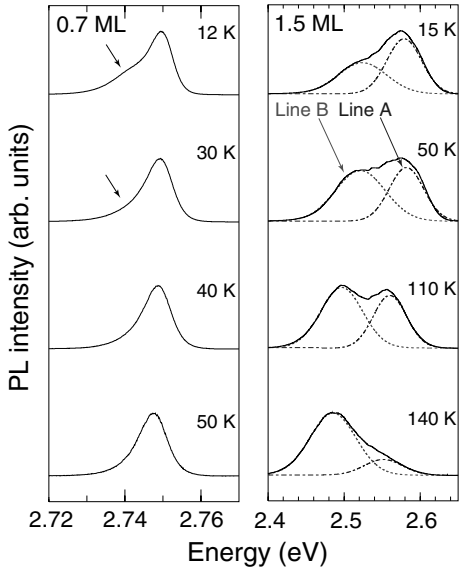

FIG. 3. Macrophotoluminescence data taken on CdSe/ZnSe samples with 0.7 and 1.5 monolayer coverages at several temperatures.

spectrum observed for 1 monolayer coverage, the emission line is qualitatively similar. However, the width of the low-energy tail is now significantly greater, as is the number of spikes, indicating an increasing number of compositional fluctuations in the x-y plane as CdSe coverage increases.

Although the spectrum for 1.5 monolayer coverage at first sight does not look much different, temperature studies of its macrophotoluminescence reveal a significant difference in the behavior observed for samples with the higher CdSe coverages. This difference is illustrated in Fig. 3, which shows photoluminescence spectra obtained for samples with 0.7 and 1.5 monolayer coverage at several temperatures. For 0.7 monolayer coverage the low-energy tail disappears quickly with increasing temperature due to thermalization of states localized on the weak fluctuations within the 2D platelets. Similar behavior is also observed for all samples with coverages up to 1 monolayer. For samples with coverages of 1.5 monolayers and higher, however, the temperature dependence of the emission spectrum suggests the emergence of a new mechanism. The right column of Fig. 3 clearly indicates that the photoluminescence spectrum observed for these higher coverages is composed of *two* distinct lines, each having very different temperature characteristics. We observe that the intensities of the two lines comprising the spectrum change rather dramatically with temperature relative to one another. At the lowest temperature the higher-energy line (which we will call line A) is clearly dominant relative to its low-energy partner (line B), while the opposite is true at high temperatures. This difference between lines A and B suggests their different origins. Specifically, the survival of line B over line A in the 1.5 monolayers sample suggests that line B is due to excitons confined to QDs seen in Fig. 1. We thus suggest that line A, with its much faster temperature decay (a behavior typical for 2D-confined excitons, as compared to 0D excitons) corresponds to emission from the 2D platelets seen in the STEM image.

To corroborate this hypothesis, we modeled the luminescence for 1.5, 1.9, and 2.6 monolayer coverages as a superposition of two Gaussian lines, and followed the temperature dependence of their linewidth. Dotted curves in Fig. 2 show a two-line fit to the data observed on the 1.5 and 1.9 monolayer samples. The luminescence observed on the sample with the highest CdSe coverage (2.6 ML) is symmetric, and can be modeled quite satisfactorily with a single line. Figure 4 shows the FWHM of lines A and B as a function of temperature for the sample with CdSe coverage of 1.9 monolayers. Again, we see the difference in the behavior between the two lines. The FWHM for the lower-energy line (B) initially shows significant narrowing as the temperature increases in the region below $\sim$60 K. Such narrowing has been observed in other QD systems, and has been ascribed to a redistribution of carriers to lower-energy QD states [21,22]. The higher-energy line (A) of the 1.9 monolayer sample shows a behavior typical of the emission of excitons confined in a quantum well, where the FWHM increases monotonically with temperature.

Based on the above optical data we conclude that, for CdSe coverages below 1.5 monolayer, only one type of emission is observed, characteristic of a 2D system. This emission is from the 2D platelets clearly revealed in the STEM images. For samples with 1.5 and 1.9 monolayer coverages, we simultaneously observe emissions from 3D quantum dots (line B) and from the 2D platelets (line A), which again is consistent with the STEM image shown in

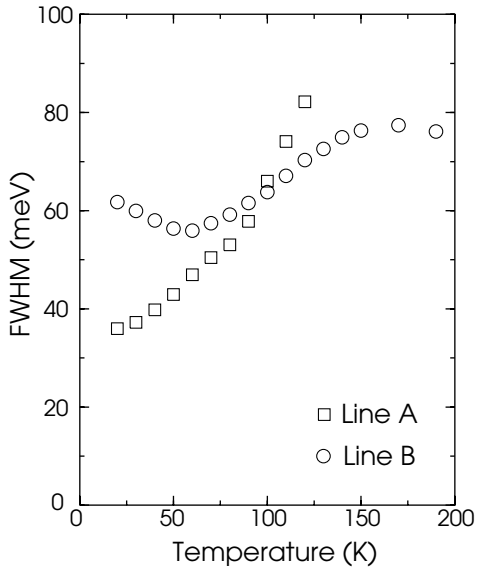

FIG. 4. Temperature dependence of full width at half maximum of line *B* (circles) and line *A* (squares) observed for the sample with 1.9 monolayer coverage of CdSe.

Fig. 1(a). The pronounced changes in the relative intensities of lines *A* and *B* as the coverage changes from 1.5 to 1.9 monolayers indicate a rapid increase in the 3D dot density, at the expense of the 2D platelets. The sample with 2.6 monolayer coverage shows only one type of luminescence, corresponding to fully developed quantum dots.

In conclusion, we have performed both photoluminescence and STEM studies on a series of samples consisting of CdSe layers of different thicknesses deposited on ZnSe, and subsequently capped. The STEM pictures give clear evidence that interdiffusion plays an important role in the process of quantum dot formation. They also show that in the early stages of the process one first observes the formation of 2D platelets, which act as precursors for the final 3D dots. The optical data fully confirm the above STEM data. These results provide strong support for the model of self-assembly proposed for quantum dots by Priester and Lannoo [9], referred to at the outset of this paper.

We thank A.-L. Barabási and J. C. Kim for helpful discussions. We acknowledge the support by the NSF (DMR-9705064, DMR-9705443, DMR-9601792, DMR-9733895, ECS-9412772) and ARO (DAAG55-97-1-0378).

*Email address: mdobrowo@nd.edu

[1] R. Notzel *et al.,* Nature (London) **369**, 131 (1994); D. Leonard *et al.,* Appl. Phys. Lett. **63**, 3203 (1993).
[2] R. Heitz *et al.,* Phys. Rev. Lett. **78**, 4071 (1997).
[3] P. B. Joyce *et al.,* Phys. Rev. B **58**, R15 981 (1998).
[4] A. S. Bhatti *et al.,* Phys. Rev. B **60**, 2592 (1999).
[5] V. A. Shchukin *et al.,* Phys. Rev. Lett. **75**, 2968 (1995).
[6] I. Daruka and A.-L. Barabasi, Phys. Rev. Lett. **79**, 3708 (1997).
[7] F. M. Ross *et al.,* Phys. Rev. Lett. **80**, 984 (1998).
[8] J. Tersoff and R. M. Tromp, Phys. Rev. Lett. **70**, 2782 (1993).
[9] C. Priester and M. Lannoo, Phys. Rev. Lett. **75**, 93 (1995).
[10] S. H. Xin *et al.,* Appl. Phys. Lett. **69**, 3884 (1996).
[11] T. Kummell *et al.,* Appl. Phys. Lett. **73**, 3105 (1998).
[12] F. Flack *et al.,* Phys. Rev. B **54**, R17 312 (1996).
[13] S. J. Pennycook and L. A. Boatner, Nature (London) **336**, 565 (1998).
[14] E. M. James and N. D. Browning, Ultramicroscopy **78**, 125 (1999).
[15] D. E. Jesson and S. J. Pennycook, Proc. R. Soc. London A **449**, 273 (1995).
[16] P. D. Nellist and S. J. Pennycook, Ultramicroscopy **78**, 111 (1999).
[17] M. Strassburg *et al.,* Appl. Phys. Lett. **72**, 942 (1998).
[18] I. L. Krestnikov *et al.,* Phys. Rev. B **60**, 8695 (1999).
[19] D. Ouadjaout and Y. Marfaing, Phys. Rev. B **41**, 12 096 (1990).
[20] B. Gil *et al.,* Phys. Rev. B **50**, 18 231 (1994).
[21] D. I. Lubyshev *et al.,* Appl. Phys. Lett. **68**, 205 (1996).
[22] Z. Y. Xu *et al.,* Phys. Rev. B **54**, 11 528 (1996).